



Knockout of beta-2 microglobulin enhances cardiac repair by modulating exosome imprinting and inhibiting stem cell-induced immune rejection

Lianbo Shao¹ · Yu Zhang¹ · Xiangbin Pan² · Bin Liu³ · Chun Liang⁴ · Yuqing Zhang¹ · Yanli Wang¹ · Bing Yan¹ · Wenping Xie¹ · Yi Sun⁵ · Zhenya Shen¹ · Xi-Yong Yu⁶ · Yangxin Li¹

Received: 30 January 2019 / Revised: 26 June 2019 / Accepted: 5 July 2019 / Published online: 16 July 2019
© Springer Nature Switzerland AG 2019

Abstract

Background and aims Allogeneic human umbilical mesenchymal stem cells (alloUMSC) are convenient cell source for stem cell-based therapy. However, immune rejection is a major obstacle for clinical application of alloUMSC for cardiac repair after myocardial infarction (MI). The immune rejection is due to the presence of human leukocyte antigen (HLA) class I molecule which is increased during MI. The aim of this study was to knockout HLA light chain β_2 -microglobulin (B2M) in UMSC to enhance stem cell engraftment and survival after transplantation.

Methods and results We developed an innovative strategy using CRISPR/Cas9 to generate UMSC with B2M deletion (B2M⁻UMSC). AlloUMSC injection induced CD8⁺ T cell-mediated immune rejection in immune competent rats, whereas no CD8⁺ T cell-mediated killing against B2M⁻UMSC was observed even when the cells were treated with IFN- γ . Moreover, we demonstrate that UMSC-derived exosomes can inhibit cardiac fibrosis and restore cardiac function, and exosomes derived from B2M⁻UMSC are more efficient than those derived from UMSC, indicating that the beneficial effect of exosomes can be enhanced by modulating exosome's imprinting. Mechanistically, microRNA sequencing identifies miR-24 as a major component of the exosomes from B2M⁻UMSCs. Bioinformatics analysis identifies *Bim* as a putative target of miR-24. Loss-of-function studies at the cellular level and gain-of-function approaches in exosomes show that the beneficial effects of B2M⁻UMSCs are mediated by the exosome/miR-24/Bim pathway.

Conclusion Our findings demonstrate that modulation of exosome's imprinting via B2M knockout is an efficient strategy to prevent the immune rejection of alloUMSCs. This study paved the way to the development of new strategies for tissue repair and regeneration without the need for HLA matching.

Keywords Exosome · Exosome's imprinting · Exosomal miRNA · Myocardial infarction · Cytotoxicity

Introduction

The use of allogeneic human umbilical mesenchymal stem cells (alloUMSCs) offers several advantages over autologous bone marrow MSCs, including better quality control, cost

effectiveness, and availability [1, 2]. However, alloUMSCs carry the risk of triggering an immune rejection, particularly in an ischemic environment, that limits their use for tissue repair [3]. Immune rejection is particularly problematic with transplanted allogeneic cells when their human leukocyte antigen (HLA) types are not matched to those of the recipient. To reduce the likelihood of rejection, recipients are often treated with immunosuppressive drugs, which have considerable adverse effects including infection [4]. Thus, immune rejection remains a major obstacle for the clinical application of alloUMSC-based therapy.

Immune rejection is mediated by the HLA molecules, which are divided into class I (HLA-I) and class II (HLA-II) antigens. The HLA-II antigens are expressed in antigen-presenting cells, such as dendritic cells, macrophages, and

Lianbo Shao, Yu Zhang, Xiangbin Pan, Bin Liu and Chun Liang have contributed equally to this work.

Electronic supplementary material The online version of this article (<https://doi.org/10.1007/s00018-019-03220-3>) contains supplementary material, which is available to authorized users.

✉ Yangxin Li
yangxin_li@yahoo.com; uuzyshen@aliyun.com

Extended author information available on the last page of the article

B cells. In contrast, HLA-I antigens are expressed in most cell types, including stem cells. HLA-I presents antigenic peptides to CD8⁺ T cells, which can attack transplanted cells. Moreover, HLA genes are highly polymorphic, which presents a challenge for matching donor and recipient for transplantation [5, 6]. HLA-I consists of a heavy-chain and a light-chain β 2-microglobulin (B2M). Disruption of the B2M gene completely disables the function of HLA-I molecules [6]. MSCs including UMSCs do not express HLA-II [7, 8], but do express HLA-I, which is upregulated in the ischemic and inflammatory milieu of infarcted myocardium. B2M ablation by CRISPR/Cas9 technology has been used to generate universal hematopoietic stem cells [9]. However, B2M has not been deleted from human UMSCs using CRISPR/Cas9, and it is not known whether B2M deletion could alter the functions of UMSCs.

The beneficial effects of MSCs including UMSCs have been attributed to the secretion of paracrine factors that are transported by exosomes [10–12]. Exosomes are membrane vesicles with a diameter between 30 and 150 nm and are known to transport functional proteins, mRNAs, and microRNAs (miRNAs) [13–15]. MSC-derived exosomes have been shown to improve heart function after myocardial infarction (MI) [16–19]. However, the underlying mechanisms, including the role of miRNAs in mediating the effects of exosomes, are not fully known. MiR-24 positively regulates cardiac functions [20, 21], but it is unknown whether exosomes contain miR-24, and whether it plays a role in exosome-mediated cardiac repair. Likewise, it is not known whether deletion of the B2M gene could alter exosome's imprinting and enhance the beneficial miR-24 mediated paracrine effects of UMSCs.

In this study, we developed an innovative strategy to generate human alloUMSCs in which the B2M gene was knocked out (B2M⁻UMSCs) using CRISPR-Cas9 technology, and investigated the effects of genetically modified B2M⁻UMSCs on immune rejection and cardiac repair in a rat model of MI.

Materials and methods

Harvest and identification of UMSC exosomes

Human umbilical mesenchymal stem cells (UMSCs) derived from Wharton's jelly of the cord (purchased from Jiangsu Heze Biotechnology Co., Ltd., China) were cultured in Dulbecco's modified Eagle's medium/F12 containing 20% fetal bovine serum (FBS) that had been centrifuged at 100,000g to eliminate preexisting bovine-derived exosomes. After 48 h of culture, exosomes were isolated from the supernatant using a total exosome isolation kit (Life Technologies) that yields large quantities of purified exosomes. The medium

from UMSC cultures was centrifuged at 2000g for 30 min to remove dead cells and debris, and then transferred to a new tube containing 0.5 volumes of the Total Exosome Isolation reagent. The mixture was incubated at 4 °C overnight and centrifuged at 10,000g for 1 h at 4 °C. The pellets were re-suspended in phosphate-buffered saline (PBS) and stored at – 80 °C. The protein concentration of UMSC exosomes was determined using a BCA protein assay kit (Takara). The morphology of UMSC exosomes was revealed by transmission electron microscopy, and the phenotype was analyzed by flow cytometry and Western blot. Because exosomes are too small to be directly captured by flow cytometry, they were attached to aldehyde/sulfate latex beads (4 μ m; Molecular Probes; Invitrogen) to amplify the signal. The pre-bound exosomes were incubated with a fluorescein isothiocyanate-conjugated antibody against CD63 (catalog ab18235, clone MEM-259, Abcam), a specific marker for exosomes, and the protein expression level of CD63 was assessed by flow cytometry. The diameter distribution of exosomes was also analyzed by Nanosight.

MI induction and implantation of UMSCs and UMSC exosomes

All animals were from the Experimental Animal Center of Soochow University (Suzhou, China), and the animal experiments were approved by the Animal Care and Use Committee of Soochow University. MI was induced in male Sprague–Dawley rats (260–280 g) as previously reported [22–25]. Animals were anesthetized by intraperitoneal injection of 80 mg/kg pentobarbital, and then the neck and chest areas were shaved. A chest retractor was positioned within the fourth intercostal space. After exposing the left ventricle, the left anterior descending (LAD) coronary artery was ligated with an 8–0 nylon suture. Successful induction of MI was verified by an immediate color change in the infarcted area. After the LAD was ligated, PBS (100 μ L), UMSCs (1×10^6 cells), B2M⁻UMSCs (1×10^6 cells), or B2M⁻UMSCs exosomes (100 μ g/100 μ L) were injected into two different sites along the infarct border. In sham control rats, the procedure was identical except that the LAD was not ligated. Penicillin (1.5×10^5 U/mL) was delivered (i.p.) after surgery.

Cardiac function

Under anesthesia (1.0% inhaled isoflurane), cardiac function was evaluated at 1, 7, 14, 28, 42, 56 days after MI by echocardiography using a 21-MHz transducer (Visual Sonics). The left ventricular ejection fraction was calculated as previously described [26]. All procedures and analyses were performed by a researcher who was blinded to the treatment groups.

B2M knockout

We constructed a lentivirus expressing CRISPR/Cas9 and a CRISPR guide RNA targeting *B2M* (forward: GACCGA GTCACATGGTTCACACGGC; reverse: AAACGCCGT GTGAACCATGTGACTC). The lentivirus particles were transfected into UMSCs.

Luciferase reporter assays

The 3'UTR of the *Bim* gene was amplified by PCR and inserted into the firefly luciferase reporter psiCHECK^{TM-2} vector (Promega). The primers used for *Bim* 3' UTR were forward: CCGCTCGAGCTGTGTCGATGTGGACGGAA, reverse: TTGCGGCCGCAGGGCAACGCCATACTCTTC. The miR-24 overexpression vector LV3-miR-24 was constructed by inserting the miR-24 sequence S: *GATCCGT GGCTCAGTTCAGCAGGAACAGTTCAAGAGACTGTTC GCTGAAGTGAAGCCACTTTTTTG*, AS: *AATTCAAAA AGTGGCTCAGTTCAGCGAACAGTCTCTTGAAGTGT CCTGCTGAAGTGAAGCCACG* into the LV3 vector (LV3: pGLV-H1-GFP + Puro Vector). HEK293T cells were co-transfected with 200 ng psiCHECK^{TM-2} vector-3' UTR and 600 ng LV3-miR-24 vector in 24-well plates for 48 h using Lipofectamine 2000. The activity of firefly and *Renilla* luciferase was analyzed using a dual-luciferase reporter assay kit (Promega) according to the manufacturer's instructions.

Western blot

Protein samples were extracted from UMSCs or exosomes using RIPA buffer with a protease inhibitor cocktail (Beyotime Biotechnology, Shanghai, China). The concentrations of protein in the samples were determined using a BCA protein assay kit (TaKaRa). Equal amounts of protein were separated by SDS-polyacrylamide gel electrophoresis and then transferred to PVDF membranes. The membranes were blocked with 5% bovine serum albumin (BSA) for 1 h at room temperature and then incubated with primary antibodies followed by a horseradish peroxidase-conjugated secondary antibody. The primary antibodies were against B2M (1:5000, catalog ab75853, clone EP2978Y, Abcam, Inc.) and Bim (1:1000, catalog ab32158, clone Y36, Abcam, Inc). All proteins were visualized with an ECL chemiluminescence kit and luminescence was measured with a BioRad luminescent imaging system.

Electron microscopy

Exosomes were re-suspended in PBS, placed on a formvar-coated copper grid, and incubated for 30 min as previously described [27]. The grid was washed with PBS and samples were fixed in 2% paraformaldehyde for 10 min. The samples

were washed several times with deionized water and then incubated with 2% uranyl acetate for 15 min. Samples were embedded in a drop of 0.13% methyl cellulose and 0.4% uranyl acetate for 10 min. The grid was examined in a JEOL JEM 1230 transmission electron microscope and images were captured by a CCD digital camera.

Loading miR-24 mimic into exosomes

The loading of exosomes with miRNA-24 mimic or scrambled mimic was based on a previously optimized protocol [27, 28]. Briefly, re-suspended exosomes were diluted in P1 primary cell solution (Lonza, USA) to a final concentration of 1 µg/µL. The human miRNA-24 mimic (RiboBio, Guangzhou, China) or scrambled miRNA mimic control (500 pmol) was added to a 200 µL sample containing 1 µg/µL exosomal protein. The mixture was transferred into a cold electroporation cuvette and electroporated according to the human MSC electroporation protocol using a 4D-NucleofectorTM System (Lonza). Immediately after electroporation, the mixture was treated with one unit of RNase A (Takara, Tokyo, Japan) for 30 min to degrade the free-floating miRNA mimic. RNase A was then deactivated by adding 2 µL RNase inhibitor (Takara) and exosomes were re-isolated using a Total Exosome isolation kit (Life Technologies) following the manufacturer's instructions. The final pellet (exosomes) was re-suspended in PBS, divided into 100-µL aliquots, and stored at -80 °C.

MicroRNA and DNA quantification

Total RNA from UMSCs, B2M⁻UMSCs, and their respective exosome preparations were extracted using TRIzol reagent (Life Technologies). RNA concentrations were verified using a spectrophotometer (NanoDrop). Equal amounts of RNA (1 µg) were reverse-transcribed using the Revert Aid First Strand cDNA Synthesis Kit (Thermo Scientific). Bulge-loopTM miRNA qRT-PCR primer sets (one RT primer and a pair of qPCR primers per set) specific for has-miR-24, cel-miR-39, and U6 were designed by RiboBio. The expression levels of miRNAs were determined by qRT-PCR with Takara SYBR Premix Ex Taq in a Stepone Plus Real-Time PCR system (Applied Biosystems). C_t values for cells were averaged and normalized to the U6 RNA, and C_t values for exosomes were averaged and normalized to the cel-miRNA-39 [29]. All experiments were repeated at least three times. Relative expression was determined using the $\Delta\Delta C_t$ comparative threshold method. Genomic DNA was isolated from rat myocardium using the Genomic DNA isolation Kit, and PCR was performed to determine the expression of Alu (with 200 ng genomic DNA template per sample).

Synthesis and administration of miR-24 inhibitor

The miR-24 inhibitor was designed and synthesized as unconjugated and fully phosphorothiolated oligonucleotides by RiboBio. miR-24 inhibitor or negative control (scrambled locked nucleic acid oligonucleotide) at a final concentration of 100 nM was transfected into B2M⁻UMSCs for 48 h using Lipofectamine 2000.

ELISA

Serum TNF- α level was determined by ELISA following the manufacturer's instructions (TNF- α ELISA kit: ThermoFisher Scientific).

Cytolytic assay

Cytolytic assays were performed as previously described [6]. Briefly, CD8⁺ T cells were isolated from human peripheral blood mononuclear cells by Ficoll density-gradient centrifugation followed by further purification using a CD8⁺ T cell isolation kit (StemCell Technologies, Vancouver, Canada). The cells were cultured in RPMI 1640 containing 10% FBS with 50 U/mL human IL-2 for 48 h prior to assay. The cytotoxic activity of CD8⁺ T cells against UMSCs and B2M⁻UMSCs was assessed using a cytotoxicity detection kit (Roche Applied Science, Indianapolis, IN). The UMSCs and B2M⁻UMSCs were re-suspended at 2×10^6 /mL in assay medium, and 100 μ L cell suspension was added to each well of a 96-well plate. CD8⁺ T cells in 100 μ L of assay medium were then added and mixed with the target cells at various effector/target (*E/T*) ratios (25:1, 12.5:1, 6.25:1, and 3.125:1). After co-culture for 3 h, the 96-well plates were centrifuged at 250 *g* for 10 min, and the supernatant was transferred to new 96-well plates, mixed with 100 μ L reaction mixture, and incubated for 30 min at room temperature. The reaction was terminated and the absorbance of the samples was detected at 490 nm.

Immunofluorescence staining of CD8, complement C3 and CD68

For immunofluorescence staining, the remainder of the heart was soaked in 20% sucrose solution for 4 h, embedded in OCT and kept in -80 °C freezer. Frozen sections (5 μ m) were incubated with rabbit anti-CD8 antibody (1:100; catalog bs0648R, Bioss Inc., Woburn, MA, USA) or rabbit anti-complement C3 antibody (1:100; catalog A00168-1, Boster Biological Technology, Wuhan, China), or mouse anti-CD68 antibody (1:200, ab31630, Abcam) overnight at 4 °C. After washing, the sections were incubated with goat anti-rabbit

IgG (ab150077, Alexa Fluor[®] 488, Abcam) or goat anti-rabbit IgG-FITC (sc2010, SANTA) at 2 μ g/mL for 1 h. The sections were finally incubated with DAPI to stain nuclei.

Immunofluorescence staining of HLA-I

UMSCs and B2M⁻UMSCs were fixed in 4% PFA for 30 min at room temperature and then blocked with 5% BSA in PBS for 1 h at room temperature. The cells were incubated with mouse anti-human HLA class I mAb (catalog ab22432, clone W6/32, Abcam, Inc) at 1:100 in 5% BSA overnight at 4 °C. After washing, the cells were incubated with the secondary antibody goat anti-mouse IgG (ab150113, Alexa Fluor[®] 488, Abcam) at 2 μ g/mL for 1 h at room temperature. Nuclei were stained with DAPI.

Statistical analysis

The data are expressed as the mean \pm SEM. Multiple comparisons were analyzed by ANOVA with post hoc analysis by the Newman-Keuls test. A two-tailed t-test was used to determine the significance of differences between two groups. $P < 0.05$ was considered statistically significant.

Results

Generation and characterization of B2M⁻UMSCs

MSCs do not express HLA-II [7, 8], but do express HLA-I. The latter is increased in the ischemic and inflammatory milieu after MI. Disruption of the *B2M* gene completely disables the function of HLA-I [6]. Thus, in order to knock out the *B2M* gene and generate alloUMSCs that are resistant to immune rejection for clinical applications, we constructed recombinant lentiviruses expressing CRISPR/Cas9 and a CRISPR guide RNA targeting the *B2M* locus (forward: GACCGAGTCACATGGTTCACACGGC; reverse: AAA CGCCGTGTGAACCATGTGACTC) (Fig. 1a). Transduction of UMSCs with the recombinant viruses led to successful ablation of the *B2M* gene (*B2M*⁻UMSCs). Efficient ablation of *B2M* was confirmed by Western blot analysis (Fig. 1b). Importantly, knockout of *B2M* did not alter the expression of the MSC markers CD90 and CD105 (Fig. 1c) and the cells retained the typical spindle-shaped morphology (Fig. 1d). Expression of HLA-I was analyzed by flow cytometry and immunostaining, which showed that it was expressed in UMSCs but not in B2M⁻UMSCs (Fig. 1e, f). Treatment with interferon gamma (IFN- γ), a typical pro-inflammatory cytokine that is known to induce HLA-I expression [30], induced HLA-I expression in UMSCs, but not in B2M⁻UMSCs (Fig. 1e, f).

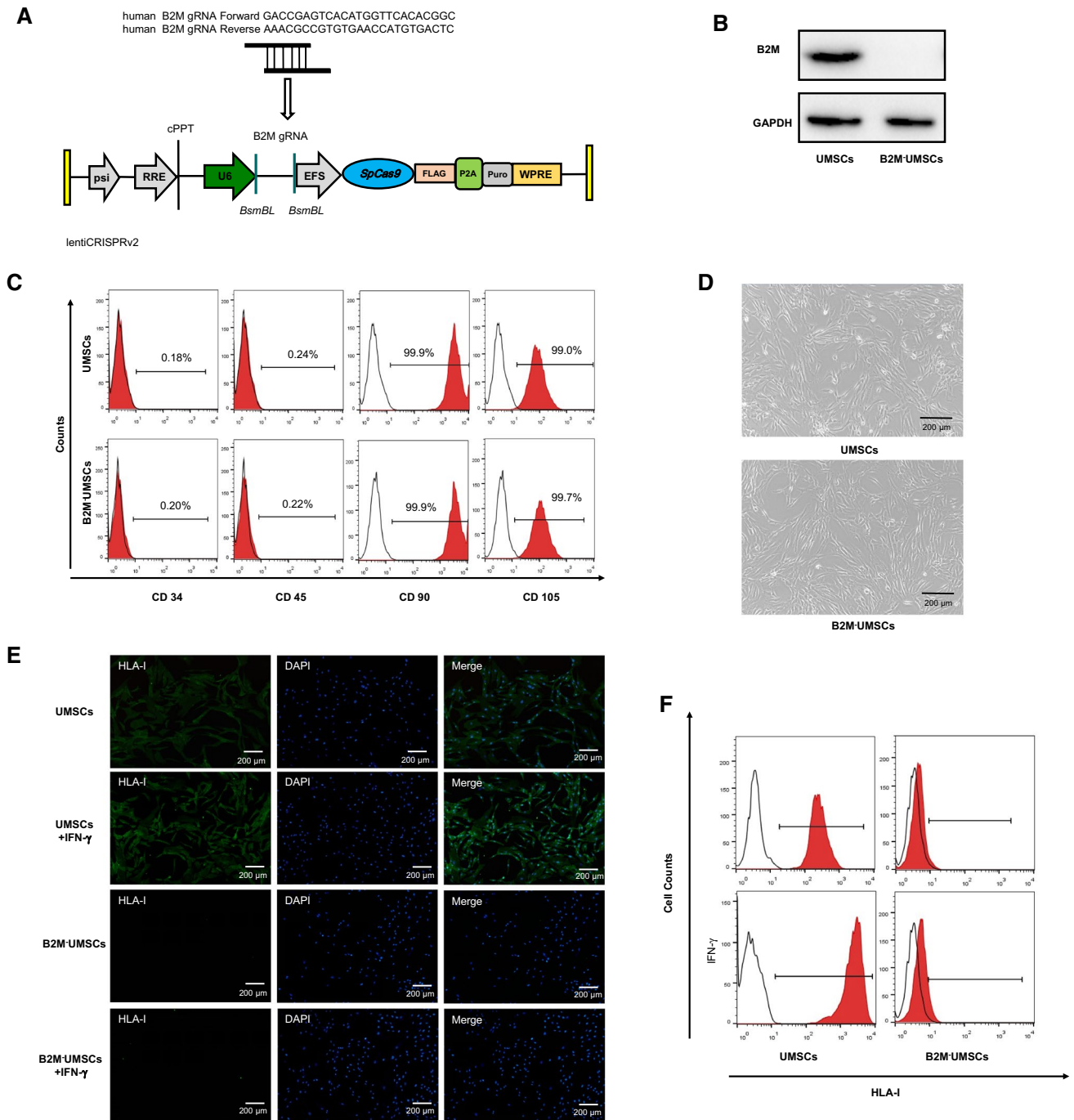


Fig. 1 Generation and characterization of B2M⁻UMSCs. **a** Schematic diagram of the recombinant lentiCRISPRv2 plasmid targeting B2M. **b** Western blots of B2M expression in UMSCs with B2M-knockout. **c** Flow cytometric analyses showing that UMSCs and B2M⁻UMSCs were both positive for CD90 and CD105, but negative for CD34 and CD45. **d** B2M⁻UMSCs and UMSCs showed similar morphol-

ogy under an optical microscope (scale bars, 200 μ m). **e** Positive immunofluorescence staining of HLA-I expression on the surface of UMSCs, but not on the surface of B2M⁻UMSCs with and without IFN- γ . **f** Flow cytometric analysis of HLA-I expression in UMSCs and B2M⁻UMSCs with and without IFN- γ (25 ng/mL)

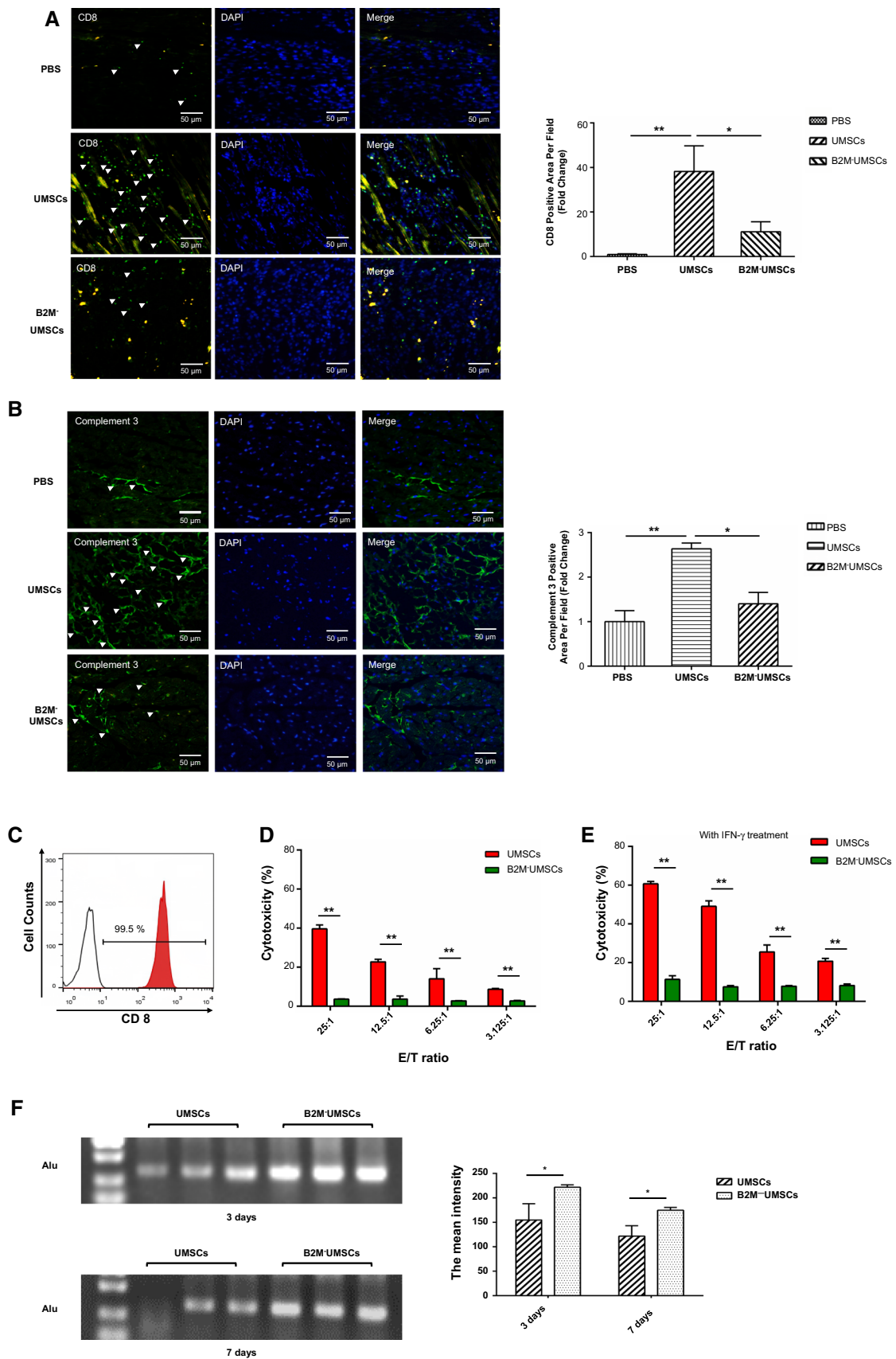


Fig. 2 B2M-knockout in UMSCs inhibits immune rejection. **a** Left panel: representative immunofluorescence staining showing numerous CD8⁺ T cells infiltrating into UMSC-injected hearts, but CD8⁺ T cells were rare in the B2M⁻UMSC-injected hearts (scale bars, 50 μm). Right panel: summary of CD8⁺ staining ($n=3$; $*p<0.05$, $**p<0.01$). **b** Left panel: representative immunofluorescence staining of a significant amount of C3 complement in UMSC-injected hearts, but little staining was found in B2M⁻UMSC-injected hearts (scale bars, 50 μm). Right panel: summary of C3 staining ($n=3$; $*p<0.05$, $**p<0.01$). **c** Flow cytometric analysis of CD8⁺ T cells isolated from human peripheral blood mononuclear cells. **d** Cytotoxicity of allogeneic CD8⁺ T cells toward UMSCs and B2M⁻UMSCs at different E/T ratios, determined by LDH release assays ($**p<0.01$). **e** LDH release assays of the cytotoxicity of allogeneic CD8⁺ T cells toward UMSCs and B2M⁻UMSCs treated with IFN-γ (25 ng/mL) ($**p<0.01$). **f** PCR analysis of the expression of Alu in rat myocardium after transplantation

Injection of alloUMSCs in immunologically competent rats induces immune rejection, which was inhibited by B2M knockout in UMSCs

Immunologically deficient animals have been used to test the functions of human stem cells [31, 32], but the effects of injecting human stem cells into an immunologically competent rat model of MI are unknown.

B2M, one component of the HLA-I molecule, is known to induce immune rejection by activating alloreactive CD8⁺ T cells. To determine whether injection of alloUMSCs induces immune rejection in immunologically competent rats and assess whether *B2M* knockout blunts the immune rejection, we injected alloUMSCs and B2M⁻UMSCs directly into the myocardium of wild-type Sprague–Dawley (SD) rats after the left anterior descending coronary artery (LAD) was ligated. ELISA assay showed that alloUMSCs induced immune reaction, but injection of B2M⁻UMSCs markedly reduced immune reaction, as evidenced by the TNF-α levels 3 days after injection (PBS = 1379 ± 169 pg/mL, alloUMSCs = 2827 ± 554 pg/mL, B2M⁻UMSCs = 1915 ± 219 pg/mL, $p < 0.05$). Moreover, injection of alloUMSCs also enhanced the recruitment of CD8⁺ T cells and the activity of complement C3 compared to the PBS-treated control group, but not in the B2M⁻UMSCs-treated group (Fig. 2a, b).

To further investigate how T cells react to allogeneic UMSCs and B2M⁻UMSCs, circulating CD8⁺ T cells were isolated from blood (Fig. 2c) and analyzed for cytotoxicity against alloUMSCs. The results showed that CD8⁺ T cells were cytotoxic to alloUMSCs at several effector cell/target (E/T) ratios, with the most vigorous killing occurring at the high concentration 25:1, but CD8⁺ T cell-mediated cytotoxicity was not observed with B2M⁻UMSCs even at the highest E/T ratio (Fig. 2d), further supporting the non-immunogenic nature of the B2M⁻UMSCs. Similarly, CD8⁺ T cell-mediated cytotoxicity was only modestly increased in B2M⁻UMSCs after treating the cells with IFN-γ (Fig. 2e). To assess the retention of the transplanted stem cells, PCR

was performed (with equal quantity template) to analyze the expression of Alu, a repeated sequence specifically expressed in primates, but not in rat [33]. The results showed that there were more B2M⁻UMSCs retained in the myocardium than UMSCs 3- and 7 days after transplantation (Fig. 2f).

To determine the impact of B2M knockout on the function of NK cells, we analyzed the expression of HLA-E and HLA-G, which inhibit immune responses by binding to receptors on NK cells. Our data showed that the expression of HLA-E was similar to that of HLA-I. B2M knockout did not alter the expression of HLA-E either in the presence or absence of IFN-γ (Suppl Fig. 1). There was no HLA-G expression on either UMSC or B2M⁻UMSCs (Suppl Fig. 2). We also analyzed the expression of ULBP3 which is a ligand that can enhance the killing activity of NK cells. The results showed that ULBP3 was not expressed on either UMSCs or B2M⁻UMSCs, even when treated by IFN-γ (Suppl Fig. 3).

Collectively, these data demonstrated that alloUMSCs, but not B2M⁻UMSCs, induce CD8⁺ T cell-mediated immune rejection in immunologically competent rats. Furthermore, B2M knockout led to better retention of the transplanted cells in the rat MI model.

Paracrine effects of B2M⁻UMSCs

The paracrine effects of UMSCs are known to be mediated by exosomes [34, 35]. To determine whether knockout of *B2M* alters the function of exosomes, we analyzed the expression levels of the exosome markers CD63 by flow cytometry, CD63 and TSG101 by Western blotting. Exosomes were isolated from the conditioned media of UMSCs and B2M⁻UMSCs, and the expression levels of CD63 and TSG101 were found to be similar between the two groups (Fig. 3a, b). Moreover, electron microscopic examination of the morphology of exosomes derived from B2M⁻UMSCs and UMSCs did not show notable differences (Fig. 3c). The distribution of the particle sizes were similar between B2M⁻UMSCs and UMSCs derived exosomes (Fig. 3d).

B2M⁻UMSCs reduces fibrosis and inflammation, and preserves myocardial function after MI

To determine whether B2M⁻UMSCs retain the full functions of UMSCs, we assessed their efficacy in restoring myocardial function in a rat model of MI. After undergoing the same surgical procedures, sex- and age-matched rats were given a single injection in the peri-infarct zone with one of the following: (1) vehicle (PBS); (2) UMSCs (1×10^6 cells/rat); or (3) B2M⁻UMSCs (1×10^6 cells/rat). Echocardiography was performed at 1, 7, 14, 28, 42 and

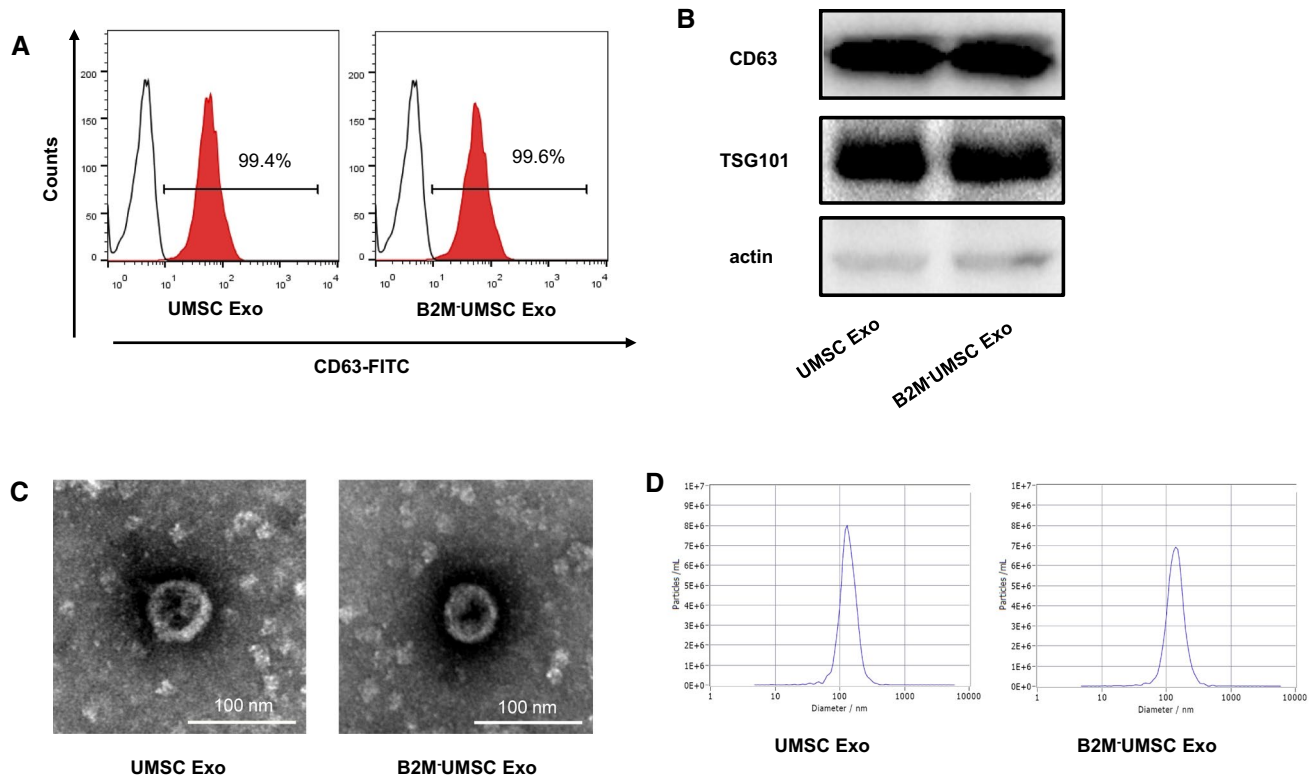


Fig. 3 Characterization of exosomes derived from UMSCs and B2M⁻UMSCs. **a** Flow cytometric analysis of the expression of the exosomes (Exo) marker CD63. **b** Western blots of CD63 and TSG101 protein in exosomes from UMSCs and B2M⁻UMSCs. **c**

Morphology of exosomes (arrows) from UMSCs and B2M⁻UMSCs revealed by transmission electron microscopy (scale bars, 100 nm). **d** Nanosight analysis the diameter size of exosomes from UMSCs and B2M⁻UMSCs

56 days after the MI. The results showed that the left ventricular ejection fraction (EF) and fractional shorting (FS) did not significantly differ among the groups at day 1 post-surgery. However, the EF and FS were markedly higher in the B2M⁻UMSC-treated and UMSC-treated groups than in the control group at 42 and 56 days after MI (Fig. 4a–c). These data showed that delivery of B2M⁻UMSCs is more effective than UMSCs to improve cardiac function in a rat model of MI.

To assess the size of the MI, thin sections of myocardium from rats injected with B2M⁻UMSCs or UMSCs were stained with Masson's trichrome 56 days after LAD ligation. As shown in Fig. 4d, the percentage of fibrotic area in the entire cross-sectional area and the percentage of fibrosis length in the entire internal circumference were both significantly lower in the groups treated with B2M⁻UMSCs or UMSCs than in the PBS group (Fig. 4e, f).

To determine whether B2M⁻UMSC treatment affects inflammation, we injected PBS, UMSCs, and B2M⁻UMSCs into the peri-infarct zone. One week after MI induction, sections were stained with anti-CD68 antibody to identify infiltrated inflammatory cells in the infarcted myocardium. CD68 expression was significantly lower in the

B2M⁻UMSC-treated group than in the PBS- and UMSC-treated groups (Fig. 4g). Based on the fact that M1 macrophages can be induced by TNF- α or IFN- γ from monocytes, and that alloUMSCs stimulated the release of TNF- α , it is possible that these CD68 positive cells are M1 macrophages.

Therapeutic effects of B2M⁻UMSCs and exosomes are mediated by miR-24/Bim

To delineate the molecular mechanisms underlying the beneficial effects of B2M⁻UMSCs and exosomes, we focused on miRNAs, which are major components of exosomes. A novel exosome-miRNA sequencing analysis was performed on the HiSeq 2500 platform and showed a marked increase in the expression levels of miR-24 (Fig. 5a). Pathway analysis indicated that the miRNAs were involved in the apoptosis signaling pathway. We selected miR-24 for further analysis for several reasons: (1) miR-24 plays critical roles in apoptosis and cardiac function; (2) the sequencing data showed that the expression of miR-24 was particularly high, which was verified by RT-qPCR (Fig. 5b); (3) real-time PCR showed

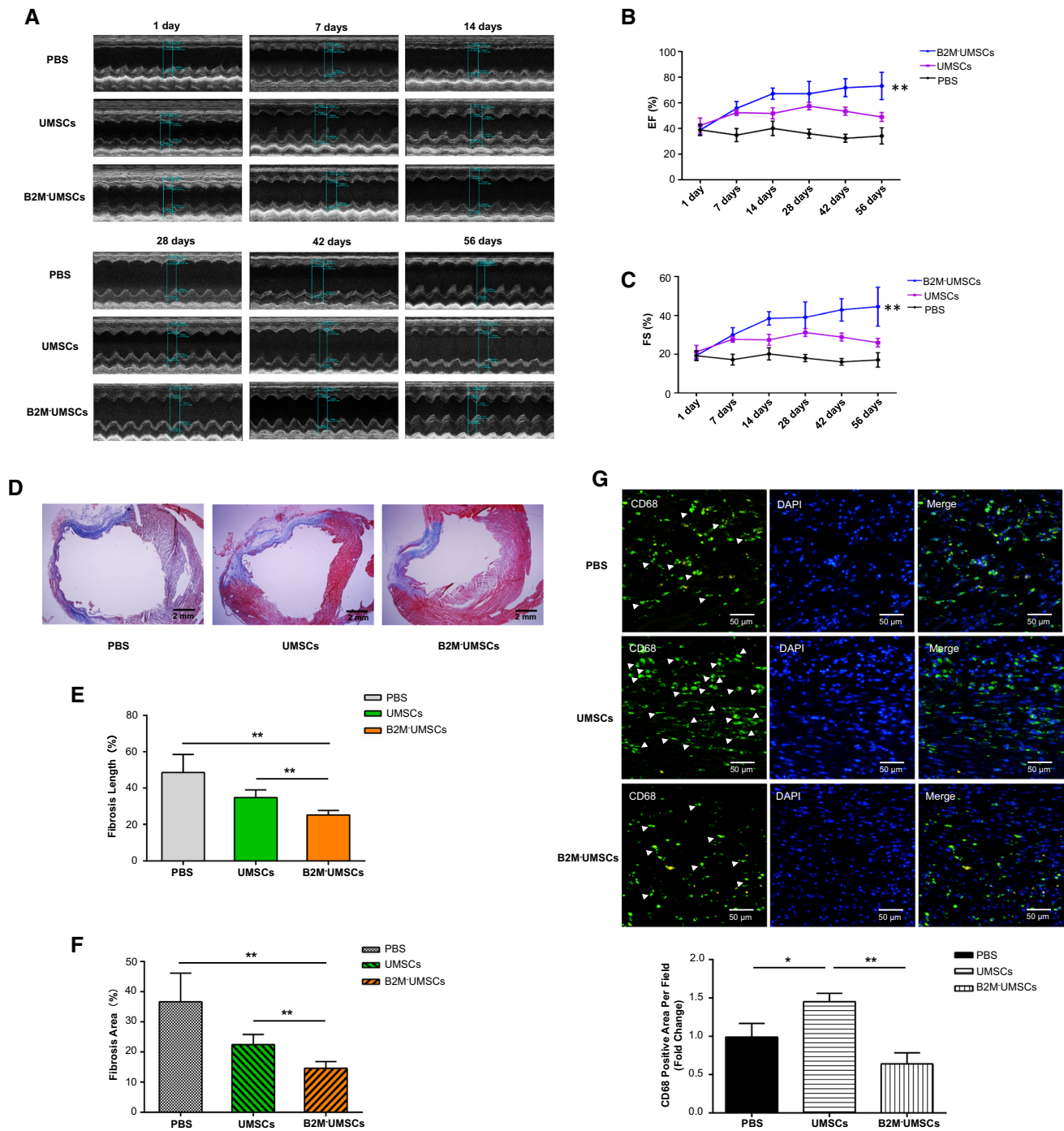


Fig. 4 B2M-UMSC treatment preserves myocardial function and reduces fibrosis and inflammation after MI. **a** Representative echocardiographic images from rats injected with PBS, UMSCs, or B2M-UMSCs. PBS, UMSCs or B2M-UMSCs were injected into the peri-infarct zone after MI induction. **b, c** EF and FS at 1, 7, 14, 28, 42 and 56 days after MI induction ($n=5/\text{group}$; UMSCs vs. B2M-UMSCs, $**p<0.01$). **d** Masson's trichrome staining of heart

sections 56 days after MI with UMSCs or B2M-UMSCs treatment (scale bars, 2 mm). **e** Quantitative analysis of fibrosis length in heart sections ($n=3$; $**p<0.02$). **f** Quantitative analysis of the area of fibrosis in heart sections ($n=3$; $**p<0.02$). **g** Upper panel: heart sections stained with anti-CD68 antibody (green) to detect inflammation in the peri-infarct zone and analyzed using ImageJ software. Lower panel: statistical summary ($n=3$; $*p<0.05$, $**p<0.01$)

higher expression of miR-24 in heart than in other rat tissues (Fig. 5c); and (4) in situ hybridization using a

locked nucleic acid probe showed miR-24 expression in the B2M-UMSCs (Fig. 5d).

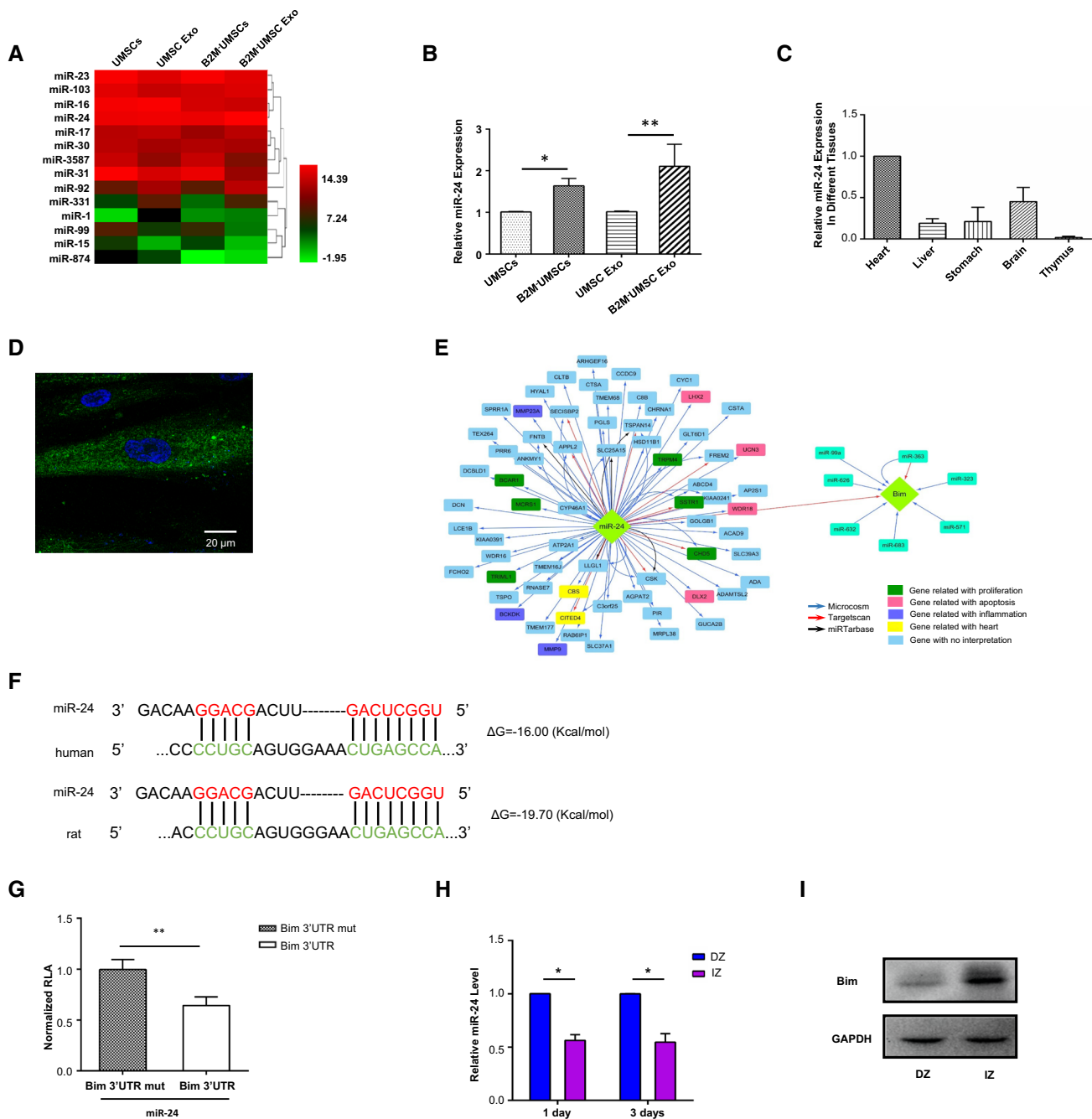


Fig. 5 Therapeutic effect of B2M-UMSCs and exosomes is mediated by miR-24/Bim. **a** Heatmap of miRNA sequencing data from UMSCs, UMSC-exosomes, B2M-UMSCs and B2M-UMSCs-exosome (green, downregulated; red, upregulated). **b** RT-qPCR analysis of miR-24 expression in cells and their derived exosomes. **c** Real-time PCR assessment of miR-24 expression in different tissues of rats. **d** In situ hybridization using a miR-24 locked nucleic acid probe in B2M-UMSCs (scale bar, 20 μ m). **e** Bioinformatics analysis identified Bim as a putative target of miR-24. **f** Tar-

getScan prediction of conserved miR-24 binding sites in the Bim 3' UTR of human and rat. Base pairs highlighted in color (miR-24 in red and Bim 3' UTR in green) are seed sequences complementary between miRNA and target. **g** Luciferase assays of HEK293T cells co-transfected with psiCHECK^{TM-2} vector-3' UTR and LV3-miR-24 vector for 48 h ($n=3$; $**p<0.01$). **h** Expression of miR-24 and Bim mRNA in the infarct zone (IZ) and distant zone (DZ) of the rat myocardium at 1 and 3 days after MI ($n=3$; $*p<0.05$). **i** Western blots of Bim expression in the IZ and DZ 3 days after MI

We used the bioinformatics tool TargetScan to identify putative targets of miR-24, which led to the identification of Bcl-2-like protein 11 (Bim) (Fig. 5e), a key protein

involved in apoptosis [27, 28, 36, 37]. Additional analysis using another bioinformatics tool, RNA22, revealed that *Bim* $\Delta G = -19.70$ kcal/mol in rat and $\Delta G = -16.00$ kcal/mol

in human (Fig. 5f), confirming *Bim* as a potential target of miR-24.

To determine whether miR-24 regulates *Bim* transcript levels, we transfected 293T cells with a plasmid expressing luciferase driven by the 3'untranslated region (UTR) of *Bim*, along with a control plasmid expressing *Renilla* luciferase (RL-TK). Luciferase assays revealed that *Bim* transcriptional activity decreased significantly in the presence of miR-24 mimic (Fig. 5g). qPCR of miR-24 and Western blot of *Bim* were performed on RNA and protein extracted from the infarct zone (IZ) and distant zone (DZ) of hearts 1 and 3 days after MI, respectively. The results showed lower expression levels of miR-24 and higher expression levels of *Bim* in the IZ than in the DZ (Fig. 5h). Western blot analysis confirmed the increased expression of *Bim* in the IZ (Fig. 5i).

To assess the role of miR-24 in cardiac repair, we performed loss-of-function studies at the cellular level and gain-of-function approaches in exosomes. We treated B2M⁻UMSCs with miR-24 inhibitor, which significantly reduced its expression in the B2M⁻UMSCs and B2M⁻UMSC exosomes compared to controls, as determined by real-time PCR (Fig. 6a). We also overexpressed miR-24 in exosomes by electroporation (Fig. 6b, c). After undergoing identical surgical procedures, sex- and age-matched rats received a single injection in the peri-infarct zone of one of the following: (1) vehicle (PBS); (2) exosomes from B2M⁻UMSC (Exo); (3) exosomes from B2M⁻UMSCs transfected with

miR-24 inhibitor (Exo + Inhib); or (4) exosomes from B2M⁻UMSCs transfected with miR-24 inhibitor + miR-24 mimic (Exo + Inhib + Mimic). The miR-24 inhibitor blocked the cardiac-protective effects afforded by the exosomes secreted by B2M⁻UMSCs (Fig. 7a). In contrast, the miR-24 mimic restored the beneficial effects of exosomes from B2M⁻UMSCs treated with the miR-24 inhibitor (Fig. 7a). EF and FS were measured at 1, 7, 14, 28, 42 and 56 days post-MI induction. Since 14 days, the EF and FS of the Exo + Inhib group were lower than those of the Exo and Exo + Inhib + Mimic groups (Fig. 7b). To assess the size of the MI, heart sections were stained with Masson's trichrome (Fig. 7c). We found that the percentage of fibrotic area in the entire cross-sectional area was significantly reduced in the Exo and Exo + Inhib + Mimic groups (Fig. 7d). Furthermore, miR-24 expression was significantly increased in hearts treated with Exo and Exo + Inhib + Mimic (Fig. 7e), whereas the expression of *Bim* was significantly decreased by Exo and Exo + Inhib + Mimic treatment (Fig. 7f).

To further investigate the contribution of the exosome-mediated miR-24/*Bim* signaling pathway in cardiac repair, we determined whether B2M⁻UMSC exosomes are internalized by myocardial cells in rats. PKH26-labeled exosomes were found on the surface of myocardial cells 1 day after injection (Fig. 8a) and in their cytoplasm 3 days after injection (Fig. 8a). PKH26-labeled B2M⁻UMSC exosomes were also internalized by H9C2 cells (Fig. 8b). H₂O₂-induced apoptosis was

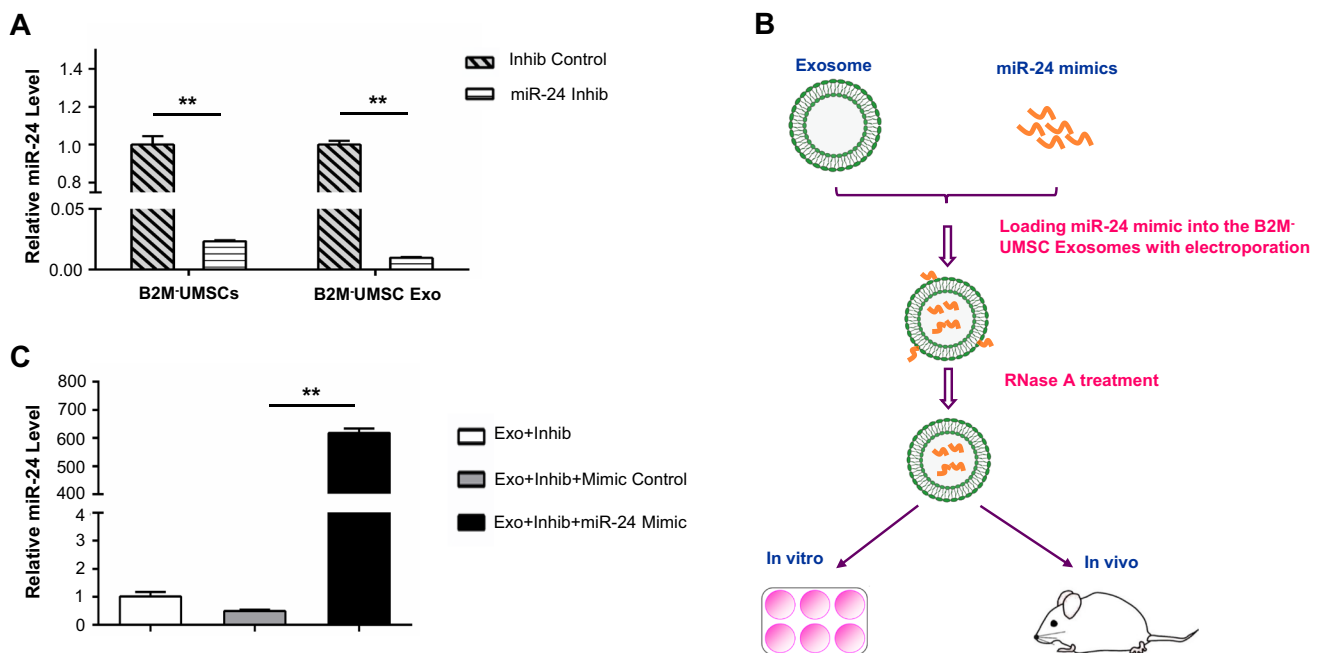


Fig. 6 miR-24 expression in cells and exosomes. **a** Real-time PCR analysis of miR-24 expression in B2M⁻UMSCs and B2M⁻UMSC exosomes (Exo) after transfection with a miR-24 inhibitor (Inhib)

(** $p < 0.01$). **b** Flowchart for loading miR-24 mimics into exosomes derived from B2M⁻UMSCs. **c** qPCR analysis of miR-24 expression (** $p < 0.01$)

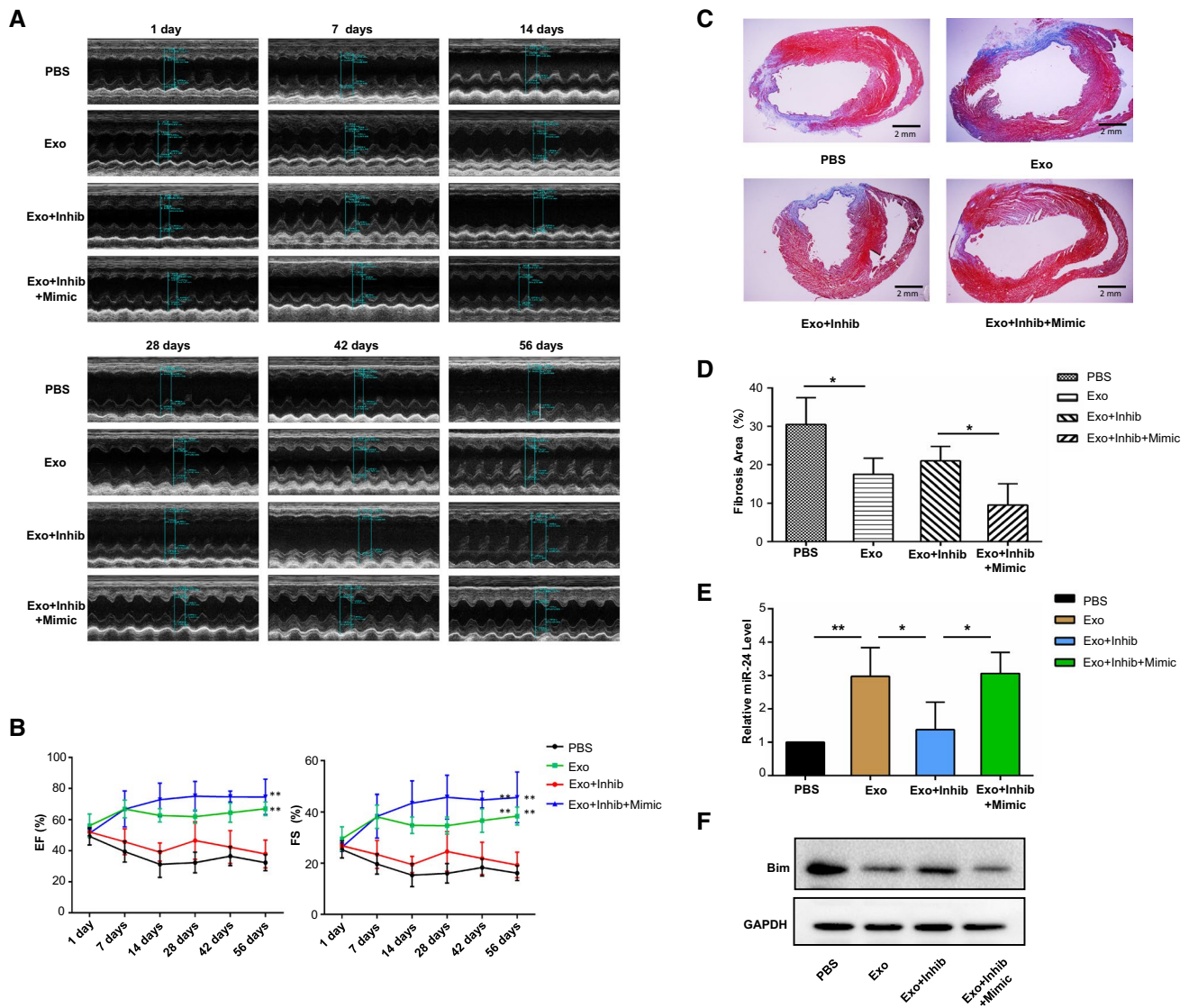


Fig. 7 Rat myocardial function after MI induction and different exosome treatments. **a** Representative echocardiographic images from rats treated with PBS, Exo, Exo+Inhib, or Exo+Inhib+Mimic. **b** EF and FS preoperatively and at 1, 7, 14, 28, 42 and 56 days after MI induction ($n=4/\text{group}$; $**p<0.01$). **c** Masson's trichrome staining in heart sections 56 days after ligation of the left anterior descending

(LAD) artery (scale bars, 2 mm). **d** Percentage of infarct zone in heart sections ($n=4$; $*p<0.02$). **e** Real-time PCR analysis of the relative expression of miR-24 in the infarct zone with different exosome treatment 3 days after LAD ligation ($n=4$, $*p<0.02$, $**p<0.01$). **f** Western blots of Bim expression in the infarcted zone

attenuated by Exo and Exo + Inhib + Mimic compared to Exo + Inhib treatment (Fig. 8c). The expression of miR-24 was increased by Exo and Exo + Inhib + Mimic (Fig. 8d), and the expression of Bim was decreased by Exo and Exo + Inhib + Mimic treatment (Fig. 8e). Moreover, B2M⁻UMSC exosomes also stimulated H9C2 cell proliferation (Fig. 8f). These data confirmed *Bim* as a direct target of miR-24 and that the beneficial effects of exosomes are mediated by the miR-24/Bim signaling pathway.

Discussion

We demonstrate that alloUMSC triggers immune rejection in wild-type SD rat with normal immune system, and our findings challenge previous opinion that alloUMSCs do not induce immune rejection [38]. Our study also reveals that knockout of HLA light chain B2M is a convenient and efficient strategy to prevent alloUMSC-induced immune rejection. Importantly, B2M⁻UMSC was more

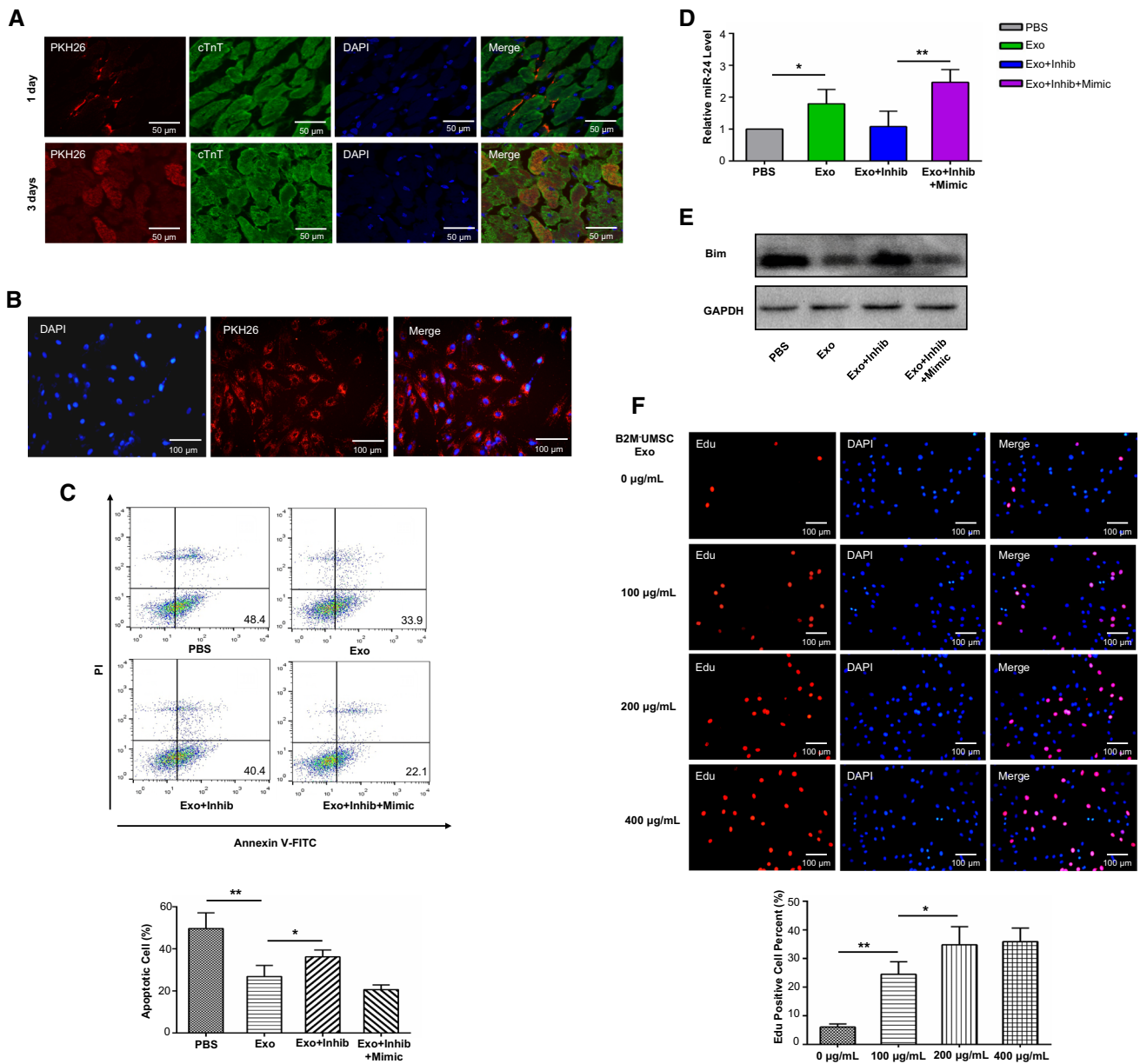


Fig. 8 MiR-24 inhibits apoptosis in H9C2 cells by downregulating Bim. **a** PKH26-labeled B2M⁻UMSC exosomes were internalized by rat myocardial cells. One day (upper panel) after intramyocardial injection of exosomes, red fluorescence was observed on the surface of myocardial cells near the injection site. Three days (lower panel) later, the red fluorescence was found in the cytoplasm of myocardial cells near the injection site. **b** Internalization of B2M⁻UMSC exosomes by H9C2 cells. PKH26-labeled B2M⁻UMSC exosomes (red) were internalized into H9C2 cells (nuclei stained with DAPI).

c Flow cytometric analysis of apoptosis induced in H9C2 cells by exposure to 200 µM H₂O₂ for 6 h and exosome treatments ($n=3$, $*p<0.05$, $**p<0.01$). **d** Real-time PCR analysis of miR-24 expression in H9C2 cells ($n=3$; $*p<0.05$, $**p<0.01$). **e** Western blots of Bim expression in H9C2 cells after B2M⁻UMSC exosome treatment following H₂O₂ induction. **f** Upper panel: representative Edu immunofluorescence staining showing B2M⁻UMSC exosomes promote proliferation of H9C2 cells in a dose-dependent manner. Lower panel: summary of Edu staining ($n=3$, $*p<0.05$, $**p<0.01$)

effective in restoring cardiac function in ischemic heart than UMSC. We further show that the beneficial effects of B2M⁻UMSC in promoting survival and repair are mediated by exosomes, which release miR-24 that targets apoptotic gene Bim in cardiomyocytes. Moreover, we demonstrate that exosomes alone can restore cardiac function,

and exosomes derived from B2M⁻UMSC are more efficient than those derived from UMSC, which indicates that exosome's function can be enhanced by modulating its imprinting.

The previous opinion that allogeneic MSCs did not induce immune rejection was based on studies using

immunodeficient animals [31, 32]. Since most MI patients are not immunodeficient, it is necessary to study the immune rejection in animal models with normal immune system. We for the first time examined the effect of alloUMSCs in a MI model using wild-type rats with normal immune system. Our findings that alloUMSCs induce immune rejection supports previous report that allogeneic MSCs are rejected in HLA-mismatched recipients [39], and highlights immune rejection as a major obstacle for clinical application of allogeneic MSCs in cardiac repair [40]. Importantly, our findings may explain the differential effects of MSC based therapy among different studies because each individual is different in terms of immune rejection. It is also possible that alloUMSC induces less severe immune rejection than other allogeneic MSCs. Thus, our findings that alloUMSC induce immune rejection suggests that other allogeneic MSC may induce even stronger immune rejection compared to alloUMSC. Therefore, the generation of HLA-deficient MSCs is the first essential step toward their clinical applications.

Although standard immunosuppressive drug prolongs the survival of transplanted stem cells, it also induces infection [41, 42]. Our strategy is based on the fact that MSCs express only HLA-I but not HLA-II antigen, and the disruption of the B2M gene can result in a complete loss of surface HLA-I expression and significant reduction of immunogenicity [6]. Our study focuses on altering MSC rather than other cell types, thus, it does not result in immune tolerance or infection.

Our findings that exosomes alone can restore cardiac function have clinical implications. The use of exosomes avoids the safety concerns and limitations associated with the transplantation of stem cells. Transplantation of exosomes reduces the immune rejection and teratoma risk associated with stem cells [43]. As a bi-lipid membrane vesicle, exosomes protect their contents from degradative enzymes or chemicals [44]. Several studies suggest that exosomes not only mimic the effects of their parent cells, but they are also influenced by the imprinting of parent cells [45]. A recent study showed that exosomes derived from human CD34⁺ stem cells improved angiogenesis and motor function in mouse ischemic limb, mimicking the effects of the parent cells. By contrast, exosomes derived from CD34⁺-cell-depleted parent cells were ineffective [32]. These results suggest that CD34⁺ stem cells contain unique molecules that are delivered specifically to endothelial cells by exosomes, and depleting CD34 alters the contents of exosomes. Our findings that exosomes derived from B2M⁻UMSC are more efficient than those derived from UMSC suggests that the modulation of exosome's imprinting is a good strategy to enhance exosome's function.

Moreover, exosomes also contain some mRNAs and microRNAs that are not functional in parent cells, but can become activated and functional in recipient cells [46]. For

example, some tumors do not express certain antigens, but exosomes can transfer antigens from tumors to dendritic cells, which in turn initiate a cytotoxic T cell-dependent immune response against tumor cells [47]. We call this phenomenon recessive exosome imprinting. It is worthwhile to explore how recessive imprinting from UMSC might influence the therapeutic effects of exosomes.

The therapeutic effects of MSC are mediated by paracrine factors which are transported by exosome [10]. Our loss of function studies at cellular level and novel gain-of-function approaches in exosomes demonstrate that B2M⁻UMSC repairs ischemic heart through exosome mediated miR-24/Bim signaling pathway. Although miR-24 has been shown to inhibit apoptosis in mouse cardiomyocytes when injected directly into ischemic myocardium in mice [36], this approach is not feasible for treating patients. We report for the first time that the delivery of exosome containing miR-24 can prevent cardiac dysfunction induced by ischemia. Because exosome can prevent miRNA degradation, the delivery strategy of miRNA by exosome has broad clinical applications. For example, miR-24 can be loaded into exosomes and delivered to target organs in vivo via intravenous injection. Furthermore, it has been shown that inflammation impairs stem cell function [48], and B2M is associated with aging [49]. Our strategy to knockout B2M reduces the levels of TNF-alpha and may also prevent stem cell senescence. Therefore, our findings provide further novel mechanistic insights into the beneficial effects of B2M⁻UMSC in addition to miR-24/Bim pathway.

Cardiac fibrosis is an unavoidable consequence of MI. Sun et al. showed that in skeletal muscle injury, miR-24 could delay the development of fibrosis by inhibiting Smad2 expression [50]. In our results, miR-24 was down-regulated in the infarcted heart, which is consistent with the findings by Wang et al. that miR-24 can inhibit TGF- β secretion and Smad2/3 phosphorylation in cardiac fibroblasts. Furin is a protease which promotes fibrosis by activating TGF- β signaling. Furin is a down stream target of miR-24. Overexpression of miR-24 could reduce the expression of Furin and inhibits the differentiation of cardiac fibroblasts. Thus, miR-24 plays a critical role in cardiac fibrosis [27]. The miRNA sequencing data showed that miR-17 and miR-92 of the miR-17-92 cluster are enriched in exosomes. miR-17-92 cluster regulates cardiomyocyte proliferation in postnatal and adult hearts [51].

In conclusion, our study demonstrates that knockout of B2M is an efficient strategy to prevent the immune rejection of alloUMSCs and enhance cardiac function through the modulation of exosome imprinting. This strategy will improve stem cell-based therapies because it can eliminate immune rejection without the need for HLA matching prior to transplantation.

Acknowledgement We thank Dr. IC Bruce for English editing of the manuscript.

Author contributions YL conceived, designed the study, analyzed data and wrote the manuscript. LS, YZ, YZ, YW, BY and WX performed the experiments and collected data. CL, BL, XP, YS, ZS and XY interpreted the data and revised the manuscript. All authors read and approved the final manuscript.

Funding This work was supported by the National Natural Science Foundation of China (NSFC, No. 81870194, No. 91849122, No. 91839101), Jiangsu Province Key Scientific and Technological Project (BE2016669), Suzhou Science and Technology Project (SS201665), Jiangsu Province Peak of Talent in Six Industries (BU24600117), National Natural Science Foundation of China (No. U1601227 to X. Y. Y.), Science and Technology Programs of Guangdong Province (No. 2015B020225006 to X. Y. Y.).

Compliance with ethical standards

Research involving animal participants The animal experiments were approved by the Animal Care and Use Committee of Soochow University.

Conflict of interest The authors declare no conflicts of interest.


References

- Karantalis V, Hare JM (2015) Use of mesenchymal stem cells for therapy of cardiac disease. *Circ Res* 116(8):1413–1430
- Landin AM, Hare JM (2017) The quest for a successful cell-based therapeutic approach for heart failure. *Eur Heart J* 38(9):661–664
- Huang XP et al (2010) Differentiation of allogeneic mesenchymal stem cells induces immunogenicity and limits their long-term benefits for myocardial repair. *Circulation* 122(23):2419–2429
- Riolobos L et al (2013) HLA engineering of human pluripotent stem cells. *Mol Ther* 21(6):1232–1241
- Rubinstein P (2001) HLA matching for bone marrow transplantation—how much is enough? *N Engl J Med* 345(25):1842–1844
- Wang D et al (2015) Targeted disruption of the beta2-microglobulin gene minimizes the immunogenicity of human embryonic stem cells. *Stem Cells Transl Med* 4(10):1234–1245
- Tan K et al (2017) Impact of adipose tissue or umbilical cord derived mesenchymal stem cells on the immunogenicity of human cord blood derived endothelial progenitor cells. *PLoS One* 12(5):e0178624
- Rink BE et al (2017) Isolation and characterization of equine endometrial mesenchymal stromal cells. *Stem Cell Res Ther* 8(1):166
- Mandal PK et al (2014) Efficient ablation of genes in human hematopoietic stem and effector cells using CRISPR/Cas9. *Cell Stem Cell* 15(5):643–652
- Sahoo S, Losordo DW (2014) Exosomes and cardiac repair after myocardial infarction. *Circ Res* 114(2):333–344
- Fang S et al (2016) Umbilical cord-derived mesenchymal stem cell-derived exosomal microRNAs suppress myofibroblast differentiation by inhibiting the transforming growth factor-beta/SMAD2 pathway during wound healing. *Stem Cells Transl Med* 5(10):1425–1439
- Qian X et al (2016) Exosomal microRNAs derived from umbilical mesenchymal stem cells inhibit hepatitis c virus infection. *Stem Cells Transl Med* 5(9):1190–1203
- Cervio E et al (2015) Exosomes for intramyocardial intercellular communication. *Stem Cells Int* 2015:482171
- Subra C et al (2010) Exosomes account for vesicle-mediated transcellular transport of activatable phospholipases and prostaglandins. *J Lipid Res* 51(8):2105–2120
- Thery C, Ostrowski M, Segura E (2009) Membrane vesicles as conveyors of immune responses. *Nat Rev Immunol* 9(8):581–593
- Teng X et al (2015) Mesenchymal stem cell-derived exosomes improve the microenvironment of infarcted myocardium contributing to angiogenesis and anti-inflammation. *Cell Physiol Biochem* 37(6):2415–2424
- Boomsma RA, Geenen DL (2012) Mesenchymal stem cells secrete multiple cytokines that promote angiogenesis and have contrasting effects on chemotaxis and apoptosis. *PLoS One* 7(4):e35685
- Lai RC et al (2010) Exosome secreted by MSC reduces myocardial ischemia/reperfusion injury. *Stem Cell Res* 4(3):214–222
- Bian S et al (2014) Extracellular vesicles derived from human bone marrow mesenchymal stem cells promote angiogenesis in a rat myocardial infarction model. *J Mol Med (Berl)* 92(4):387–397
- Guo C et al (2015) Cardiomyocyte-specific role of miR-24 in promoting cell survival. *J Cell Mol Med* 19(1):103–112
- Pan LJ et al (2017) MiR-24 alleviates cardiomyocyte apoptosis after myocardial infarction via targeting BIM. *Eur Rev Med Pharmacol Sci* 21(13):3088–3097
- Hatzistergos KE et al (2010) Bone marrow mesenchymal stem cells stimulate cardiac stem cell proliferation and differentiation. *Circ Res* 107(7):913–922
- Kawada H et al (2004) Nonhematopoietic mesenchymal stem cells can be mobilized and differentiate into cardiomyocytes after myocardial infarction. *Blood* 104(12):3581–3587
- Padin-Iruegas ME et al (2009) Cardiac progenitor cells and biotinylated insulin-like growth factor-1 nanofibers improve endogenous and exogenous myocardial regeneration after infarction. *Circulation* 120(10):876–887
- Iso Y et al (2014) Priming with ligands secreted by human stromal progenitor cells promotes grafts of cardiac stem/progenitor cells after myocardial infarction. *Stem Cells* 32(3):674–683
- Zentilin L et al (2010) Cardiomyocyte VEGFR-1 activation by VEGF-B induces compensatory hypertrophy and preserves cardiac function after myocardial infarction. *FASEB J* 24(5):1467–1478
- Wang J et al (2012) MicroRNA-24 regulates cardiac fibrosis after myocardial infarction. *J Cell Mol Med* 16(9):2150–2160
- Xiang Y et al (2015) Hyperglycemia repression of miR-24 coordinately upregulates endothelial cell expression and secretion of von Willebrand factor. *Blood* 125(22):3377–3387
- Chevillet JR et al (2014) Quantitative and stoichiometric analysis of the microRNA content of exosomes. *Proc Natl Acad Sci USA* 111(41):14888–14893
- Lu P et al (2013) Generating hypoimmunogenic human embryonic stem cells by the disruption of beta 2-microglobulin. *Stem Cell Rev* 9(6):806–813
- Deng Y et al (2016) Prostacyclin-producing human mesenchymal cells target H19 lncRNA to augment endogenous progenitor function in hindlimb ischaemia. *Nat Commun* 7:11276
- Mathiyalagan P et al (2017) Angiogenic mechanisms of human CD34(+) stem cell exosomes in the repair of ischemic hindlimb. *Circ Res* 120(9):1466–1476
- Ammar HI et al (2015) Comparison of adipose tissue- and bone marrow-derived mesenchymal stem cells for alleviating doxorubicin-induced cardiac dysfunction in diabetic rats. *Stem Cell Res Ther* 6:148
- Mayourian J et al (2018) Exosomal microRNA-21-5p mediates mesenchymal stem cell paracrine effects on human cardiac tissue contractility. *Circ Res* 122(7):933–944

35. Hu Y et al (2018) Exosomes from human umbilical cord blood accelerate cutaneous wound healing through miR-21-3p-mediated promotion of angiogenesis and fibroblast function. *Theranostics* 8(1):169–184
36. Qian L et al (2011) miR-24 inhibits apoptosis and represses Bim in mouse cardiomyocytes. *J Exp Med* 208(3):549–560
37. Maegdefessel L et al (2014) miR-24 limits aortic vascular inflammation and murine abdominal aneurysm development. *Nat Commun* 5:5214
38. Coulson-Thomas VJ et al (2014) Umbilical cord mesenchymal stem cells suppress host rejection: the role of the glycocalyx. *J Biol Chem* 289(34):23465–23481
39. Huang WH et al (2014) Hypoxic mesenchymal stem cells engraft and ameliorate limb ischaemia in allogeneic recipients. *Cardiovasc Res* 101(2):266–276
40. de Almeida PE et al (2013) Immunogenicity of pluripotent stem cells and their derivatives. *Circ Res* 112(3):549–561
41. Swijnenburg RJ et al (2005) Embryonic stem cell immunogenicity increases upon differentiation after transplantation into ischemic myocardium. *Circulation* 112(9 Suppl):I166–I172
42. Swijnenburg RJ et al (2008) Immunosuppressive therapy mitigates immunological rejection of human embryonic stem cell xenografts. *Proc Natl Acad Sci USA* 105(35):12991–12996
43. Singla DK (2016) Stem cells and exosomes in cardiac repair. *Curr Opin Pharmacol* 27:19–23
44. van Dongen HM et al (2016) Extracellular vesicles exploit viral entry routes for cargo delivery. *Microbiol Mol Biol Rev* 80(2):369–386
45. Li Y et al (2017) Dominant and recessive imprinting of exosomes from parent cells. *Nat Rev Cardiol* 14(8):491
46. Boon RA, Vickers KC (2013) Intercellular transport of microRNAs. *Arterioscler Thromb Vasc Biol* 33(2):186–192
47. Wolfers J et al (2001) Tumor-derived exosomes are a source of shared tumor rejection antigens for CTL cross-priming. *Nat Med* 7(3):297–303
48. Shahrivari M et al (2017) Peripheral blood cytokine levels after acute myocardial infarction: IL-1beta- and IL-6-related impairment of bone marrow function. *Circ Res* 120(12):1947–1957
49. Smith LK et al (2015) beta2-microglobulin is a systemic pro-aging factor that impairs cognitive function and neurogenesis. *Nat Med* 21(8):932–937
50. Sun Y et al (2018) miR-24 and miR-122 negatively regulate the transforming growth factor-beta/smad signaling pathway in skeletal muscle fibrosis. *Mol Ther Nucleic Acids* 11:528–537
51. Chen J et al (2013) mir-17-92 cluster is required for and sufficient to induce cardiomyocyte proliferation in postnatal and adult hearts. *Circ Res* 112(12):1557–1566

Publisher's Note Springer Nature remains neutral with regard to jurisdictional claims in published maps and institutional affiliations.

Affiliations

Lianbo Shao¹ · Yu Zhang¹ · Xiangbin Pan² · Bin Liu³ · Chun Liang⁴ · Yuqing Zhang¹ · Yanli Wang¹ · Bing Yan¹ · Wenping Xie¹ · Yi Sun⁵ · Zhenya Shen¹ · Xi-Yong Yu⁶ · Yangxin Li¹ 

¹ Institute for Cardiovascular Science and Department of Cardiovascular Surgery, First Affiliated Hospital of Soochow University, Suzhou 215123, Jiangsu, People's Republic of China

² Department of Cardiac Surgery, Fuwai Hospital, Beijing 100037, People's Republic of China

³ Department of Cardiology, The First Hospital of Jilin University, Changchun 130041, Jilin, People's Republic of China

⁴ Department of Cardiology, Changzheng Hospital, Second Military Medical University, Shanghai 200003, People's Republic of China

⁵ Fuwai Yunnan Cardiovascular Hospital, Kunming 650302, Yunnan, People's Republic of China

⁶ Guangzhou Medical University, Guangzhou 510080, Guangdong, People's Republic of China